Copy
RM L54E17

NACA

RESEARCH MEMORANDUM

AN EXPERIMENTAL INVESTIGATION OF TWO-DIMENSIONAL, SUPERSONIC CASCADE-TYPE INLETS AT A MACH NUMBER OF 3.11

By Edward Óffenhartz

Langley Aeronautical Laboratory
Langley Field, Va.

NATIONAL ADVISORY COMMITTEE
FOR AERONAUTICS

WASHINGTON

August 25, 1954

NATIONAL ADVISORY COMMITTEE FOR AERONAUTICS

RESEARCH MEMORANDUM

AN EXPERIMENTAL INVESTIGATION OF TWO-DIMENSIONAL, SUPERSONIC CASCADE-TYPE INLETS AT A MACH NUMBER OF 3.11

By Edward Offenhartz

SUMMARY

A preliminary investigation of two-dimensional, supersonic cascade-type inlets at a free-stream Mach number of 3.11 has been conducted at the Langley Aeronautical Laboratory. Two cascade-type inlets utilizing different methods of internal-flow compression were designed and tested. In one inlet (designated cascade inlet) the passages were contoured to generate coalesced compressions; whereas those of the other inlet (designated stepped-cascade inlet) were contoured to generate noncoalesced compressions. Pressure and Mach number distributions as well as shadowgraphs are presented for both inlets. With mass-flow ratios of 1, the maximum values of total-pressure recovery attained at 0° angle of attack were 0.43 and 0.45 for the cascade and stepped-cascade inlets respectively, as compared to a theoretical value of about 0.64 for both inlets. Individual passages of the cascade inlet attained maximum values of total-pressure recovery of 0.50. The differences between maximum total-pressure recovery for the individual passages and the entire cascade inlet are due to the losses involved in straightening the velocity profiles of the individual passages and to subsonic mixing of the air from individual passages. Both inlets were stable in the supercritical region only. The Mach number distributions obtained approximately 40 minimum widths downstream from the leading edge of the inboard passages of both inlets were fairly uniform across the passage width. Separation of the supersonic flow which increases with back pressure takes place within the individual passages of both inlets. The separation is asymmetric, and the asymmetry has no systematic relationship with back pressure.

INTRODUCTION

In the development of supersonic inlets, initial emphasis was placed on conical-type inlets. These inlets were designed to be housed within the nose of a supersonic vehicle or to be carried externally in wing pods. In both cases the inlet and engine are mounted in tandem. Analysis and

tests of conical inlets (refs. 1, 2, and 3) indicated that the large cowl-lip angles necessary in the design of conical inlets result in high values of external wave drag at Mach numbers greater than 2.5. However, recent tests of conical inlets (refs. 4 and 5) indicate that it is possible to attain high total-pressure recovery without prohibitive external drag.

To overcome effects of external wave drag associated with conical inlets operating at their design Mach numbers, two-dimensional, rectangular-scoop inlets were designed and tested, as reported in references 6, 7, and 8. These inlets are fuselage supported in such a manner so as to add less external wave drag than conical inlets. Scoop inlets so mounted (see fig. 1) direct the compressed air (after subsonic turning) to fuselage-housed engines. The inlets reported in these references attain total-pressure recovery almost as great as nose inlets.

Two-dimensional cascade-type inlets can be housed within the wing of a supersonic vehicle in such a manner as to add less external wave drag than conical inlets. Two versions of such a wing-root inlet are shown in figure 2. The leading edge of the outboard blade tip of each passage is similar to the cowl of a conical inlet. However, each of the outboard surfaces of the blades acts as a compression surface for the succeeding passage. At the design Mach number, the leading edge of the wing and the first compression for each passage are coincident. The external wave drag associated with wing-housed cascade inlets is then less than that associated with conical inlets.

In both wing-housed cascade inlets shown in figure 2 the turning of the air is accomplished supersonically with the reflected compression CF as shown in the inboard passages. Of course, if the air is not to be delivered in a streamwise direction, the strength of the reflected compression can be reduced by utilizing more cutback on the upper blade surface of each passage. If this process is theoretically carried to the limit, a cascade scoop inlet having zero thickness at the upper blade tip results, and the air is directed parallel to the compression surface. In order to maintain finite upper blade thickness, each passage must be brought forward into the free stream. The theoretical total-pressure recovery for any one passage of such a cascade scoop inlet would then correspond to the value of approximately 90 percent for the isolated scoop.

The primary purpose of this investigation was to study the starting characteristics, flow-mixing characteristics, and velocity profiles in cascade inlets. To study these characteristics, the two configurations shown in figure 2 (though not optimum pressure recovery inlets) were investigated. The data obtained included pressure distributions, total-pressure recoveries, Mach number distributions, and shadowgraphs for a Mach number of 3.11 and 0° angle of attack.

[redacted]

Dr. Antonio Ferri initiated preliminary investigation of cascade inlets while employed at the Langley Laboratory.

SYMBOLS

M_o	free-stream Mach number
M_1	subsonic-diffuser Mach number
m/m_o	ratio of measured mass flow to mass flow through a free-stream tube of cross-sectional area equal to projected inlet frontal area
p_1	local static pressure
p_b	static pressure at upstream end of orifice plate
P_o	total pressure of free stream
P_f	total pressure after diffusion
P_f/P_o	total-pressure recovery

AERODYNAMIC DESIGN OF THE CASCADE INLETS TESTED

Passage contours.- Two cascade-type inlets were designed for operation at a free-stream Mach number of 3.0. Different internal-flow compression was obtained by contouring the inlet passages. The cascade inlet passages were contoured to generate coalesced compressions; whereas those of the stepped-cascade inlet were contoured to generate noncoalesced compressions.

Consider the cascade inlet shown in figure 2(a). At the design Mach number the wing leading edge BC and the first compression generated by the surface BE at B are coincident. The flow is further compressed by turning the surface BEF such that all compressions generated coalesce at the point C. Since the surface CD is cut back from the free-stream direction by an insufficient amount to follow the streamline, a reflected compression CF results. The intensity of this compression is determined by the difference between the flow angles at C as generated by the surface BE and the cutback angle at point C.

Consider the stepped-cascade inlet shown in figure 2(b). At the design Mach number the wing leading edge BC and the first compression generated by the surface BE at B are coincident. The remaining compressions generated along the surface BE are spaced so as to generate

noncoalescing compressions. The first compression generated at the point B is reflected at the point C where the surface CD is cut back by a small amount. The remaining compressions generated by the surface BE are canceled along the surface CD.

Cascading.- Cascading results in a reduction of the axial length of the inlet and thus the cascade inlet becomes shorter than that of a single-passage inlet using identical supersonic turning. The cascade-type inlet consists of four identical passages having the required total free-stream-tube capture area. Each passage of the cascade-type inlets discharges into a common constant-area plenum chamber which serves as a mixing region. Thus each passage to this point is essentially an independent inlet.

Starting cascade-type inlets.- During the starting process of cascade or stepped-cascade inlets, the mass flow corresponding to the free-stream tube based upon the projected passage frontal area must be swallowed by each passage. The inlet is considered as started when the first compression coincides with or is within the inlet swept leading edge, the normal shock has passed the minimum, and the mass-flow ratio m/m_o is 1.

Consider an instantaneous shock position during the starting process of the stepped-cascade inlet as shown in figure 3. The initial shock is assumed to be attached at L and extended a short distance to M. At the point M a normal shock occurs. The shock is normal to the internal flow from M to N and oblique to the free-stream flow as shown by MP. The flow behind the detached shock MP is supersonic such that the oblique shock OP is attached at the point O but not coincident with the swept leading edge. The shock PR is assumed to be a strong oblique shock behind which the flow is subsonic. For the inboard passage, some flow is spilled around the inlet as indicated by the streamline TS. The flow can also be spilled to the next passage. This spillage from one passage to the next is the difference between starting the cascade inlets and single scoop inlets as discussed in references 9 and 10. If the mass flow spilled is more than that required for equilibrium, then the shock configuration will move in the downstream direction. The shock LM becomes coincident with the swept leading edge LS and the normal shock MN moves downstream past the minimum section of the inboard passage. The shock MPR becomes less oblique and the flow at the point O becomes identical to the conditions originally shown for the inboard passage. The process is repeated for this channel and the others in succession until all passages start.

It has been found experimentally that starting phenomena limited the contraction ratio to 2.38 and 2.28 for the cascade and stepped-cascade inlets, respectively. The entire starting process takes place almost instantaneously with the inboard passage starting first and the outboard passage starting last.

MODELS AND TESTS

Models.- The two models tested and their corresponding blade geometries are shown in figures 4 and 5. The leading-edge angle of the swept cover walls in the plane parallel to the free-stream direction was 6° for the cascade inlet and 12° for the stepped-cascade inlet. The increased angle for the stepped-cascade inlet was necessary in order to house glass inserts in the cover walls. These inserts enabled visual observation of the inlet internal flow.

The surfaces comprising the inboard and outboard passages of both inlets were instrumented with static- and total-pressure tubes which were installed on the blade center lines (see fig. 6). Total-pressure tubes were also installed in the subsonic mixing region. Cover-wall pressure orifices were installed at all total-pressure-tube locations for the cascade inlet. The stepped-cascade inlet had no cover-wall orifices at the passage total-pressure-tube locations because of the glass inserts. The locations of all measuring stations are shown in figure 6.

Tests and measurements.- Both inlets were tested at 0° angle of attack at a free-stream Mach number of 3.11 and Reynolds numbers of approximately 13 and 14.3×10^6, based upon the inlet height for the cascade and stepped-cascade inlets, respectively. Since both inlets had the same frontal dimensions, the difference in Reynolds number is due to stagnation pressure. The tests were conducted in a supersonic blowdown jet of the Langley Gas Dynamics Branch by using dry air supplied from high-pressure tanks. Figure 7 shows a schematic drawing of the test installation.

The tests were performed in the following manner. With the tunnel and inlet started, the throttle valve was turned from fully opened to the point where flow instability of the inlet occurred. Measurements were made at intermediary conditions up to the point just before the onset of unsteady flow. Gages and mercury manometers were used to record pressures. The mass flow through the model was measured with a calibrated orifice located upstream of the throttle valve as shown in figure 7. The differential pressure across the orifice was measured on a mercury-filled U-tube. All pressure measuring instruments were photographed. Total-temperature measurements were made upstream of the mass-flow orifice plate and in the settling chamber. Pressure measurements were estimated to be accurate within ±1 percent and result in pressure and mass-flow ratios accurate to ±2 percent.

RESULTS AND DISCUSSION

Static- and total-pressure distributions presented were obtained for inlet operation in the supercritical region only. The flow was unstable below the critical point and no attempt was made to stabilize the flow for operation in the subcritical region. The data are presented for three operating conditions denoted by the ratio p_b/P_o. For all conditions discussed the inlets were started.

At a free-stream Mach number of 3.11, if it is assumed that it is possible for a normal shock to exist just downstream of the leading edge of the outboard surface of any one passage and if subsonic losses are neglected, the estimated total-pressure recovery for any one passage is 64 percent for both inlets.

Cascade Inlet

Shadowgraphs.- The supersonic flow pattern at the entrance of the cascade inlet is shown in figure 8. It has been found experimentally that the supersonic flow at the entrance is independent of back pressure until the onset of unsteady flow. The position of the first shock is seen to be slightly different for each of the passages. This difference becomes more pronounced in the outboard direction. The disturbance "a" in figure 8(b) is weak and does not alter the flow entering the inlet.

Passage pressure distributions.- Figure 9 shows the variation of static pressure with length for both the inboard and outboard passages. The theoretical distribution for the inboard surfaces 1 and 3 of both passages is included for comparison. A value of $p_1/P_o = 0.36$ is theoretically obtainable slightly downstream of the leading edges of surfaces 2 and 4. The general flow pattern is qualitatively as follows: For values of p_b/P_o equal to 0.31 and 0.36, the flow undergoes compression to the minimum section, supersonic expansion beyond this point, and further compression downstream. For p_b/P_o equal to 0.41 there is compression from the inlet leading edge up to the last measuring station.

The difference in pressure ratio at the first measuring station for surfaces 1 and 3 is due to the local flow angularity which is estimated to be $+1/2^\circ$. For values of p_b/P_o equal to 0.31 and 0.36 the decrease in measured pressure ratio beyond the minimum section is due to the cutback of surfaces 1 and 3.

The differences between the inboard- and outboard-passage flows are largely due to boundary-layer separation. Figure 10 presents the varia-

tion of cover-wall static-pressure (p_l/P_o) and total-pressure recoveries (P_f/P_o) with passage width. Regions of separation $(p_l/P_o \geq P_f/P_o)$ are apparent. There is asymmetric separation from all surfaces of the inboard and outboard passages, and the asymmetry has no systematic relationship with back pressure.

The weighted total-pressure recovery (weighted with respect to mass flow throughout this report) is 50 percent for both end passages when p_b/P_o is equal to 0.41. This result is obtained under the assumption that the mass flow through the separated region is zero and that the static pressure measured on the cover wall and the total pressure measured on the blade center line are constant across the passage height.

Plenum-chamber-pressure measurement.- Figure 11 presents the total-pressure recoveries obtained in the subsonic plenum chamber at the rake location. The outboard portion of the plenum chamber indicates higher values of total-pressure recovery. This increase is probably due to the difference of flow travel before reaching the measuring station and is associated with less mixing losses. There is no distinguishable wake effect of the inboard blades at the measuring station. The weighted total-pressure recovery is 43 percent when p_b/P_o is equal to 0.41.

Comparison of the weighted total-pressure recovery attained by the individual inboard and outboard passages with that attained in the plenum chamber indicates the magnitude of the losses due to straightening the individual passage profiles as well as the mixing of the four subsonic streams.

The Mach number distribution shown in figure 12 is reasonably uniform, considering the separation which was present within the individual passages as indicated in figure 10.

Stepped-Cascade Inlet

Passage pressure distributions.- Figure 13 presents the variation of pressure with length for both the inboard and outboard passages of the stepped-cascade inlet. The theoretical distributions are included for comparison. The general flow pattern for all operating conditions is similar to that described for the cascade inlet.

The inboard-surface pressure distribution for both passages near the leading edge is lower than theoretical. The difference is due to the local flow angularity of $+1/2^{\circ}$. In figure 13(a) the pressure distribution for inboard surface 1 as measured is in agreement with theory until the minimum section. For all values of p_b/P_o, the decrease in pressure

ratio beyond the minimum section is due to flow expansion around the cutback surface 1. In the absence of sufficient data, the data for inboard surface 3 shown in figure 13(b) are arbitrarily faired to show compression from the point beyond the minimum up to the last measuring station.

Figure 14 shows the variation of total-pressure recoveries with passage width. The surface values are those obtained from the pressure distributions shown in figure 13. There is asymmetric separation from all surfaces of the inboard and outboard passages, and the asymmetry has no systematic relationship with back pressure.

Shadowgraphs.- The supersonic flow pattern at the entrance of the stepped-cascade inlet as well as the internal flow in the passages is shown in figure 15 for the values of p_b/P_o indicated. The disturbance "b" emanates from the lower nozzle block and extends around the inlet. It is partially visible through the glass inserts in the nozzle cover walls and should not be considered in analyzing the passage internal flow.

Figure 15(b) clearly shows the difference in the separation of the supersonic flow along the inboard surfaces of passages A and B. The expansion at the upstream portion of the inboard surfaces of both passages is due to the cutback of these surfaces. The portion of the internal flow visible for the third passage is similar to that of passages A and B.

Increasing p_b/P_o moves the region of supersonic flow separation forward on all the inboard surfaces as shown in figure 15(c). The flow in all passages is similar, with separation of the supersonic flow taking place asymmetrically.

The flow pattern in passages A and B of figure 15(d) can be conjectured as follows: In passage A the flow is subsonic with the possibility of supersonic flow along the outboard surface. The main supersonic flow region has moved upstream beyond the window. The flow in passage B consists of a supersonic region along the outboard surface of the passage and a highly turbulent subsonic region. As p_b/P_o increases there is no indication of the occurrence of a systematic normal shock pattern.

Detailed correlation between the flow pictures as determined from the shadowgraphs of figure 15 and the pattern which can be inferred from the pressure profiles is difficult. The data of figure 14(b) are taken along the passage center line, whereas the shadowgraphs of figure 15 are pictures through the entire passage and present a composite three-dimensional-flow effect.

[redacted]

Plenum-chamber-pressure measurement.- Figure 16 shows the variation of total-pressure recovery across the width of the plenum chamber at the measuring station. The increase of total pressure in the outboard direction is probably due to the difference in flow travel before reaching the measuring station. The weighted total-pressure recovery is 45 percent when p_b/P_o is equal to 0.43. The Mach number distributions shown in figure 17 are relatively uniform over the passage width.

CONCLUSIONS

An investigation has been made of two-dimensional cascade-type supersonic inlets at a free-stream Mach number of 3.11 and 0° angle of attack. Two inlets utilizing different methods of internal-flow compression were designed and tested to study primarily starting characteristics, mixing characteristics, and velocity profiles in cascade inlets. In one inlet (designated cascade inlet) the passages were contoured to generate coalesced compressions; whereas, those of the other inlet (designated stepped-cascade inlet) were contoured to generate noncoalesced compressions. The following results were obtained from this investigation:

1. The starting phenomenon of cascade inlets is such that each cascade starts by allowing spillage to the sides of the inlet and over the succeeding cascade blades. Starting takes place almost instantaneously with the inboard passage starting first and the outboard passage starting last. Both inlets were stable in the supercritical region only.

2. With mass-flow ratios of 1, the maximum values of total-pressure recovery obtained were 0.43 for the cascade inlet and 0.45 for the stepped-cascade inlet, as compared to a theoretical value of about 0.64 for both inlets. Individual passages of the cascade inlet attained maximum values of total-pressure recovery of 0.50. The differences between maximum total-pressure recovery for the individual passages and the entire cascade inlet are due to the losses involved in straightening the velocity profiles of the individual passages and to subsonic mixing of the air from the individual passages. Higher total pressure recoveries could probably be obtained in cascade-type inlets if the inlets were not required to deliver air in the streamwise direction as in the case of the designs tested.

3. The Mach number distributions obtained approximately 40 minimum widths downstream from the leading edge of the inboard passages of both inlets were fairly uniform across the passage width.

4. Separation of the supersonic flow which increases with back pressure takes place within the individual passages of both inlets. The separation is asymmetric, and the asymmetry has no systematic relationship with back pressure.

Langley Aeronautical Laboratory,
National Advisory Committee for Aeronautics,
Langley Field, Va., May 6, 1954.

REFERENCES

1. Oswatitsch, Kl.: Pressure Recovery for Missiles With Reaction Propulsion at High Supersonic Speeds (The Efficiency of Shock Diffusers). NACA TM 1140, 1947.

2. Ferri, Antonio, and Nucci, Louis M.: Theoretical and Experimental Analysis of Low Drag Supersonic Inlets Having Circular Cross Section and a Central Body at Mach Numbers of 3.30, 2.75, and 2.45. NACA RM L8H13, 1948.

3. Ferri, Antonio, and Nucci, Louis M.: Preliminary Investigation of a New Type of Supersonic Inlet. NACA Rep. 1104, 1952. (Supersedes NACA TN 2286.)

4. Connors, James F., and Woollett, Richard R.: Force, Moment, and Pressure Characteristics of Several Annular Nose Inlets at Mach Number 3.85. NACA RM E53J09, 1954.

5. Hunczak, Henry R.: Pressure Recovery and Mass-Flow Performance of Four Annular Nose Inlets Operating in Mach Number Region of 3.1 and Reynolds Number Range of Approximately 0.45×10^6 to 2.20×10^6. NACA RM E54A07, 1954.

6. Comenzo, Raymond J., and Mackley, Ernest A.: Preliminary Investigation of a Rectangular Supersonic Scoop Inlet With Swept Sides Designed for Low Drag at a Mach Number of 2.7. NACA RM L52J02, 1952.

7. Anon.: Design and Analysis of Three Supersonic Side Inlet Diffuser Models. Wright Aero. Rep. No. 1755 (Contract No. AF 33(600)8733 Item 28, S.A. No. 1), Curtiss-Wright Corp., Wright Aero. Div. (Wood-Ridge, N. J.), Sept. 22, 1953.

8. Anon.: Quarterly Progress Report on Ramjet Development. Wright Aero. Rep. No. 1711 (Contracts AF33(038)-9000 and AF33(600)-8733), Curtiss-Wright Corp., Wright Aero. Div. (Wood-Ridge, N. J.), Apr. 6, 1953.

9. Himka, Theodore: Methods of Starting Scoop-Type Inlets. Wright Aero. Rep. No. 1692, Supersonic Inlet Symposium, Curtiss-Wright Corp. (Wood-Ridge, N. J.), Jan. 23, 1953.

10. Ferri, Antonio: Recent Developments in the Design of Supersonic Scoop Diffusers. Wright Aero. Rep. No. 1692, Supersonic Inlet Symposium, Curtiss-Wright Corp. (Wood-Ridge, N. J.), Jan. 23, 1953.

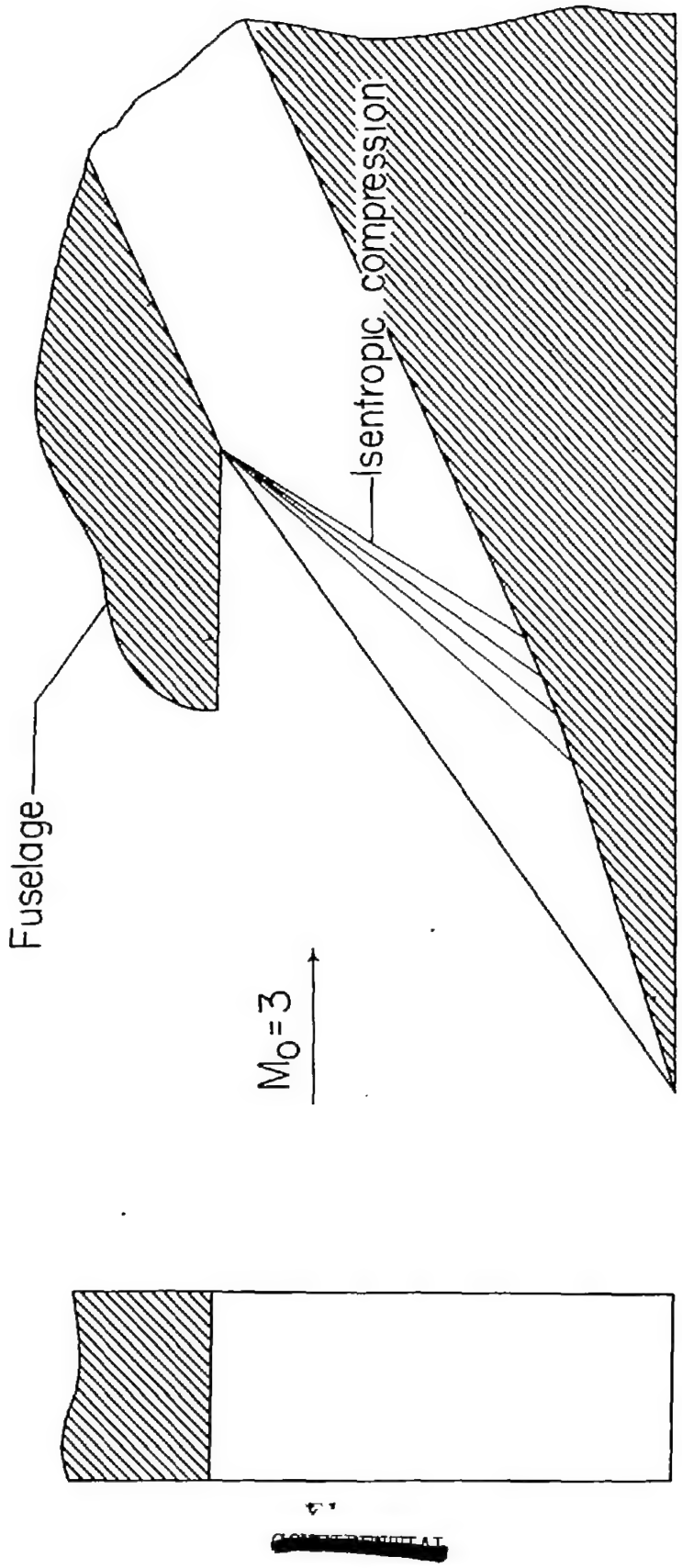

Figure 1.- Two-dimensional scoop inlet.

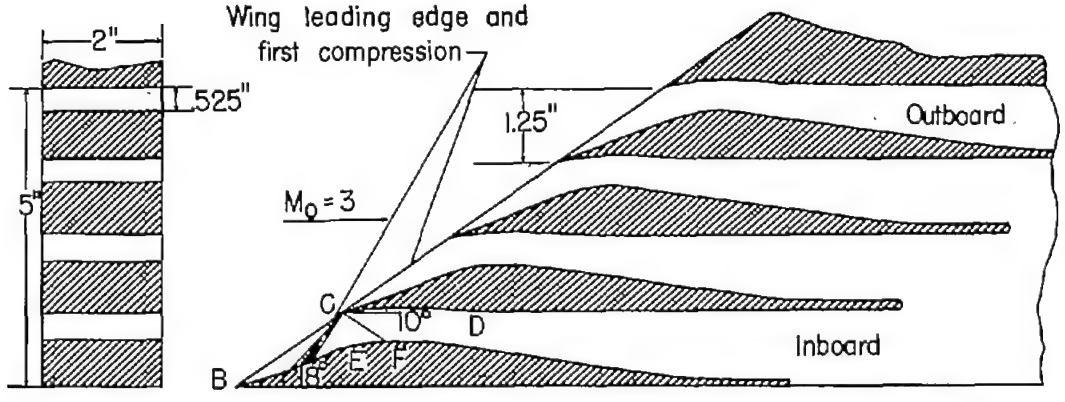

(a) Cascade inlet.

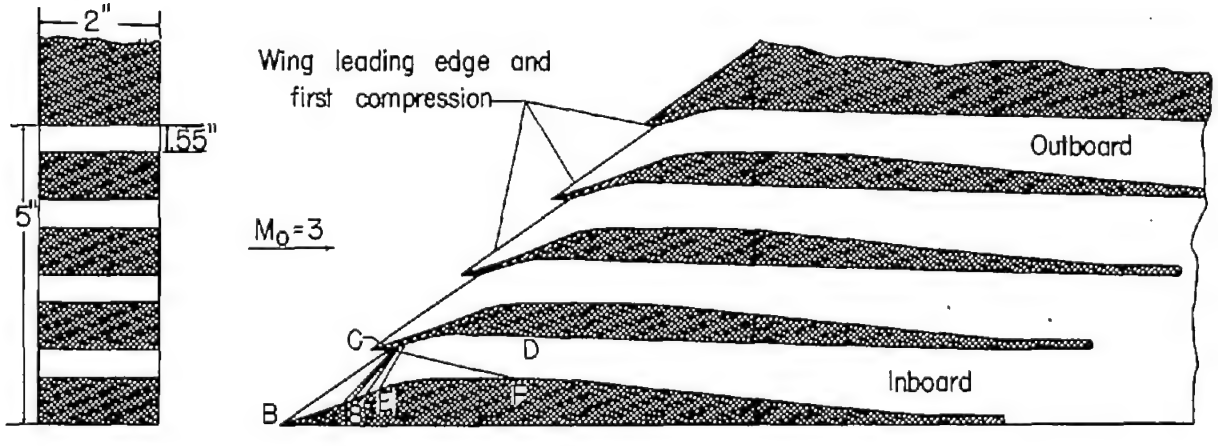

(b) Stepped-cascade inlet.

Figure 2.- Two-dimensional cascade-type inlets.

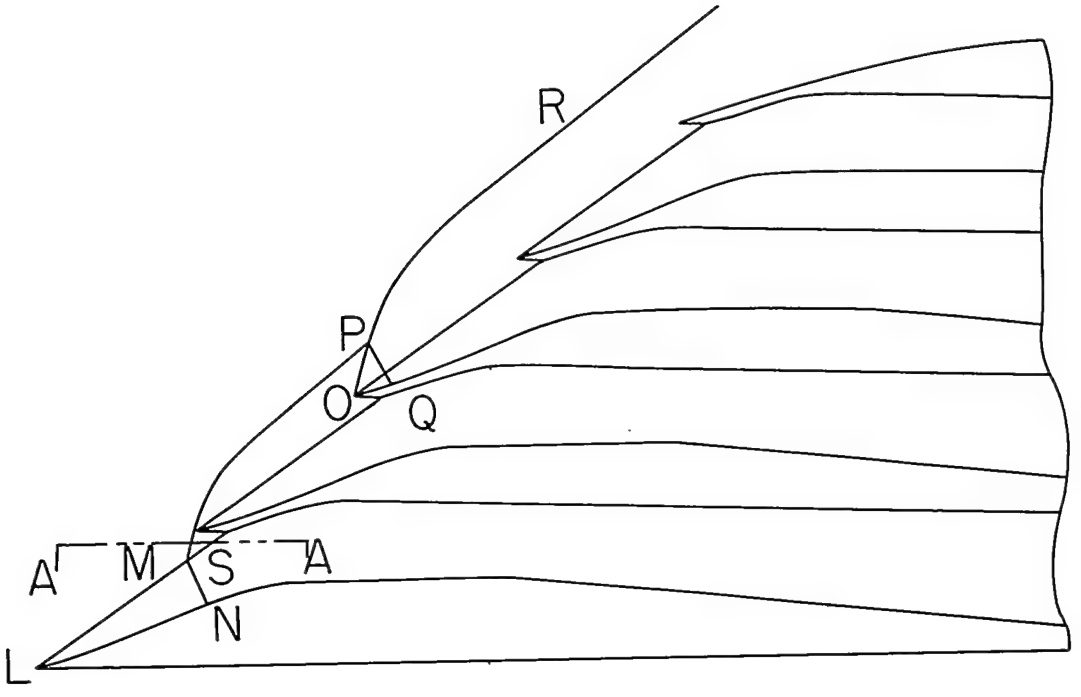

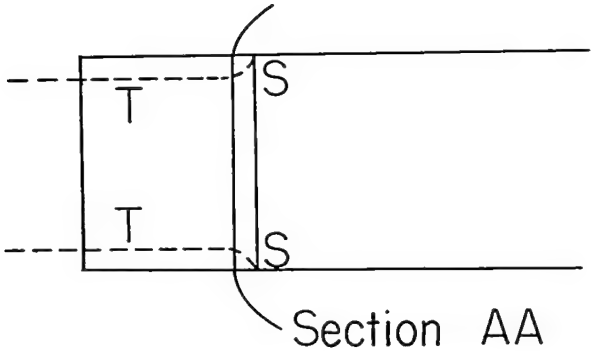

Figure 3.- Starting process of stepped-cascade inlets.

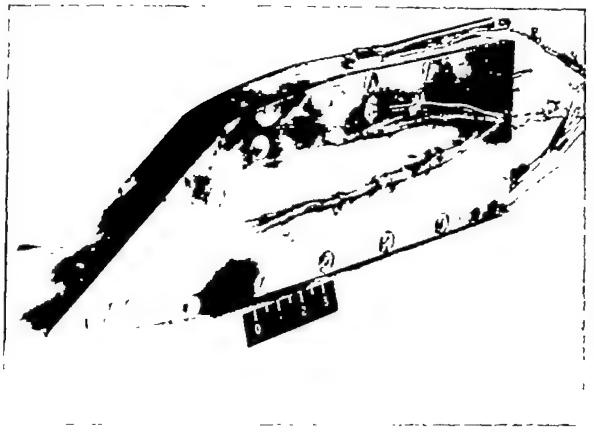

L-82229

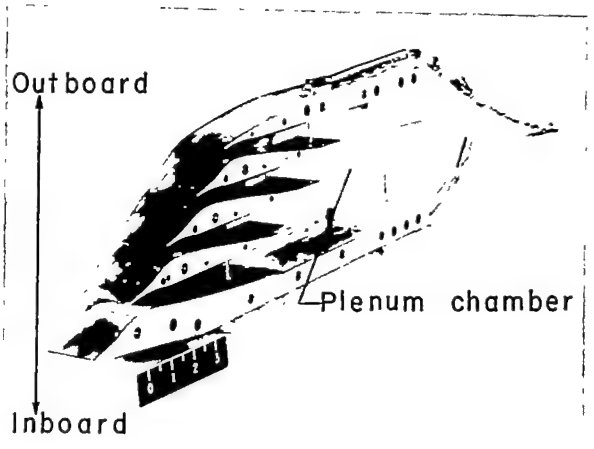

L-82232.1

X	Y_L	X	Y_U
0	0	0	0
.125	.021	.625	.210
.200	.037	.875	.290
.246	.041	1.000	.336
.300	.053	1.250	.446
.355	.060	1.370	.504
.440	.075	1.500	.560
.500	.082	1.635	.610
.555	.088	1.750	.660
.700	.100	1.875	.700
.800	.107	2.000	.740
.900	.110	2.124	.768
1.000	.120	2.375	.800
1.125	.110	2.550	.809
1.250	.107	2.752	.810
1.370	.100	3.000	.795
1.500	.092		
1.635	.080		
1.750	.064		
1.875	.055		
2.000	.048		

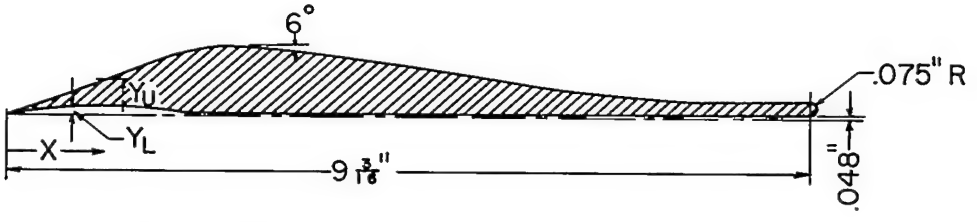

Figure 4.- Cascade-inlet blade geometry.

[redacted]

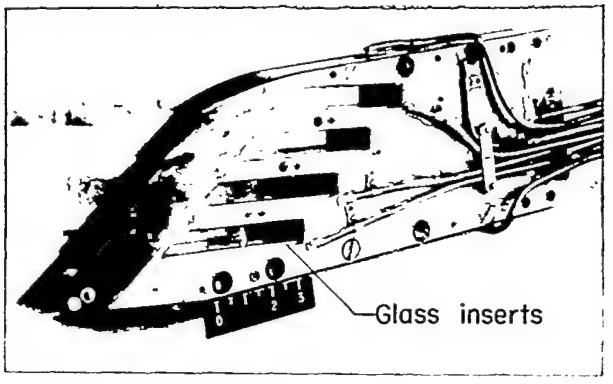

L-82227.1

X	Y_L	X	Y_U
0	0	0	0
.176	.035	1.035	.340
.235	.045	1.240	.415
.376	.088	1.412	.485
.506	.126	1.650	.595
.646	.184	1.910	.696
.700	.200	2.000	.720
.800	.225	2.200	.758
.900	.240	2.344	.775
1.000	.250	2.475	.780
1.100	.252	4.300	.780
1.200	.255		

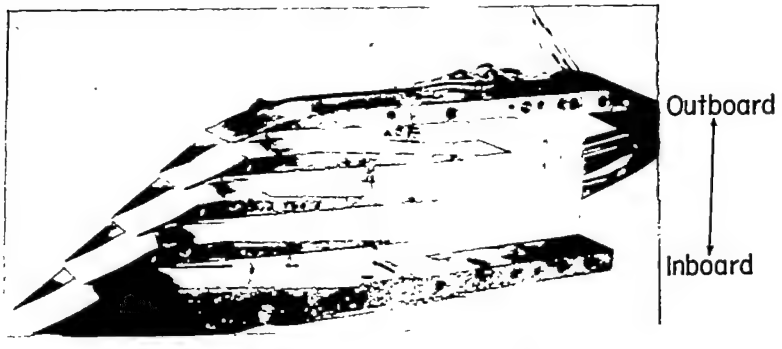

L-82231.1

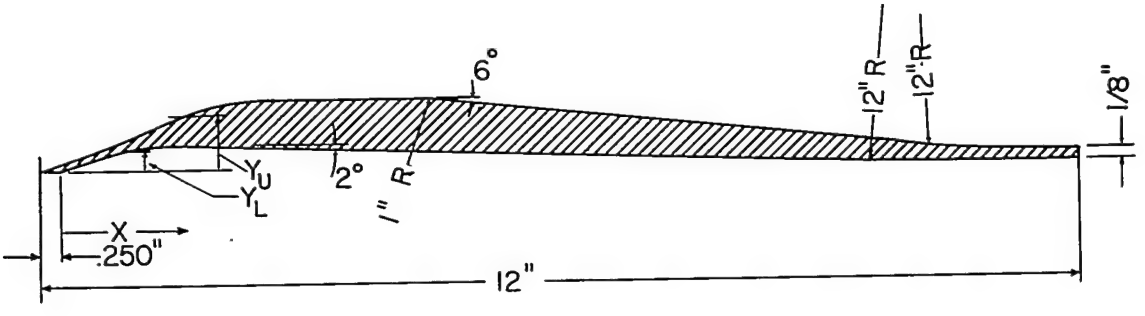

Figure 5.- Stepped-cascade-inlet blade geometry.

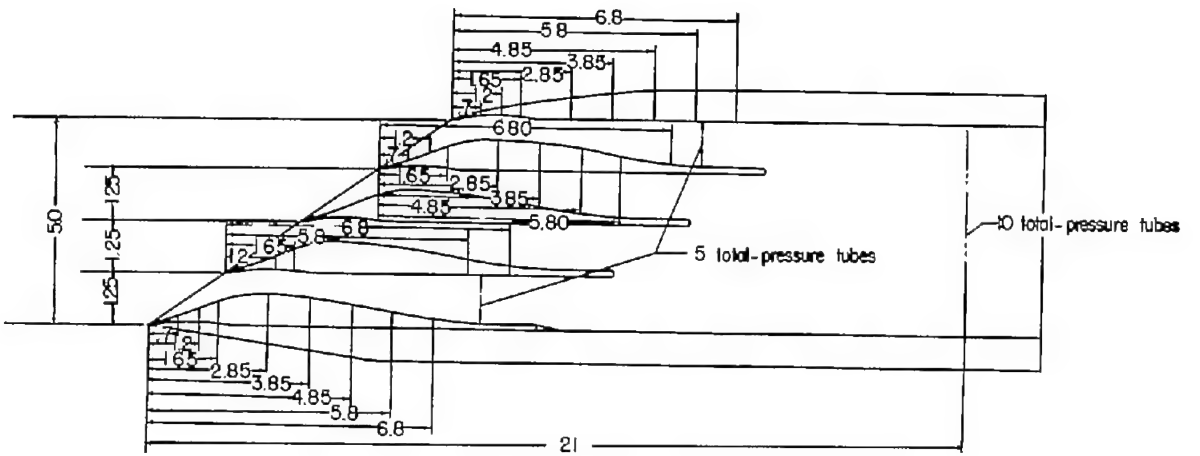

(a) Cascade inlet.

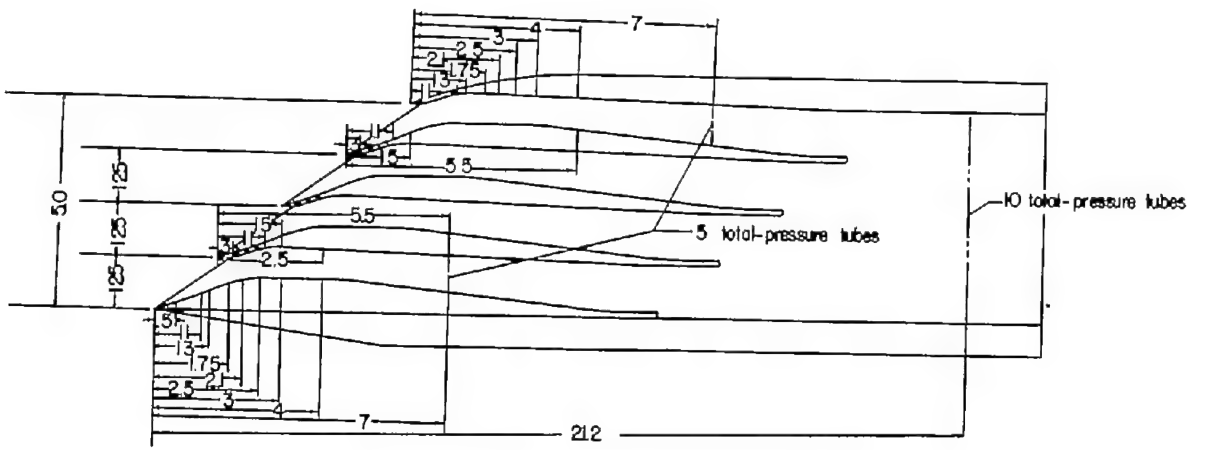

(b) Stepped-cascade inlet.

Figure 6.- Location of measuring stations. (All dimensions are in inches.)

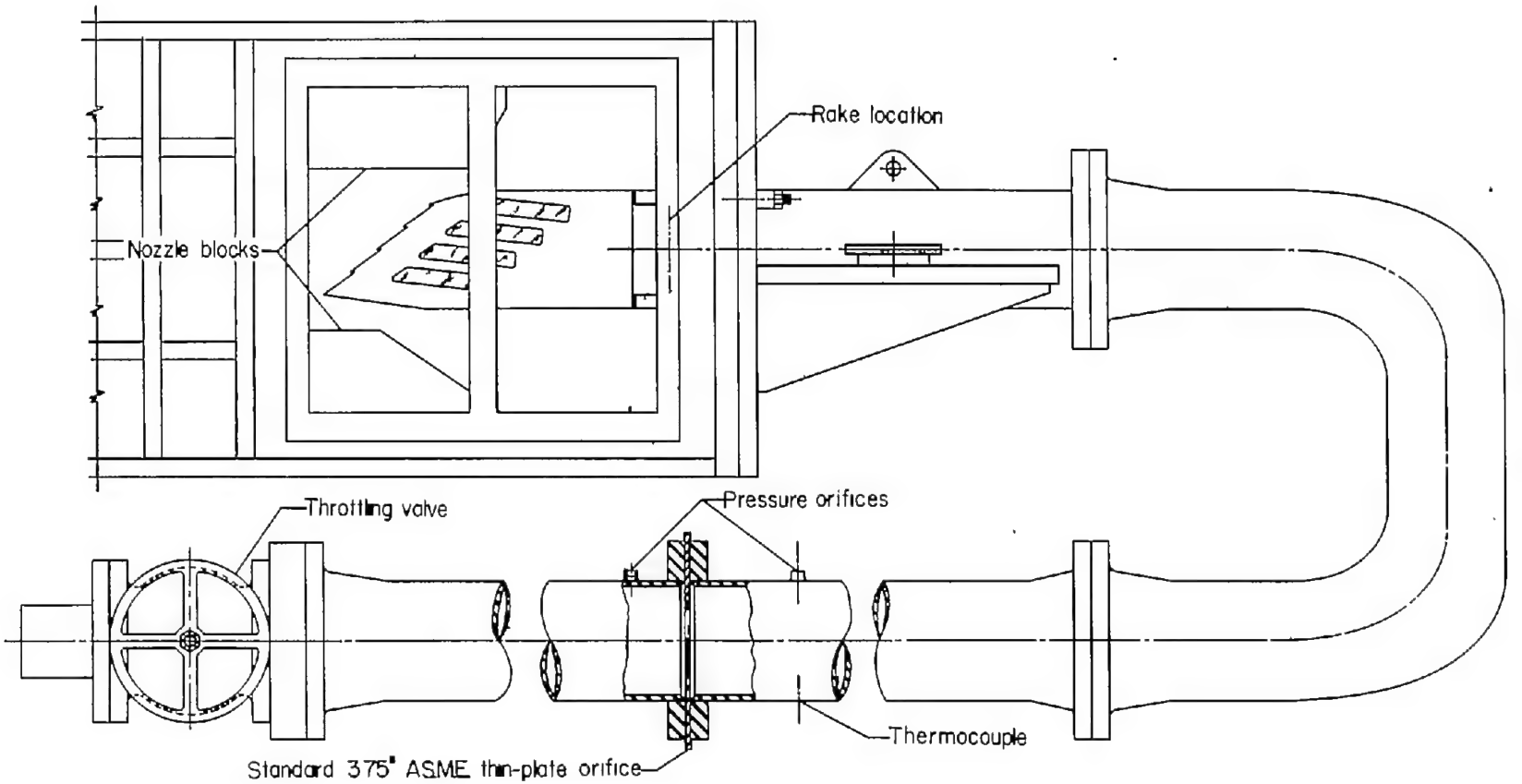

Figure 7.- Schematic drawing of test installation.

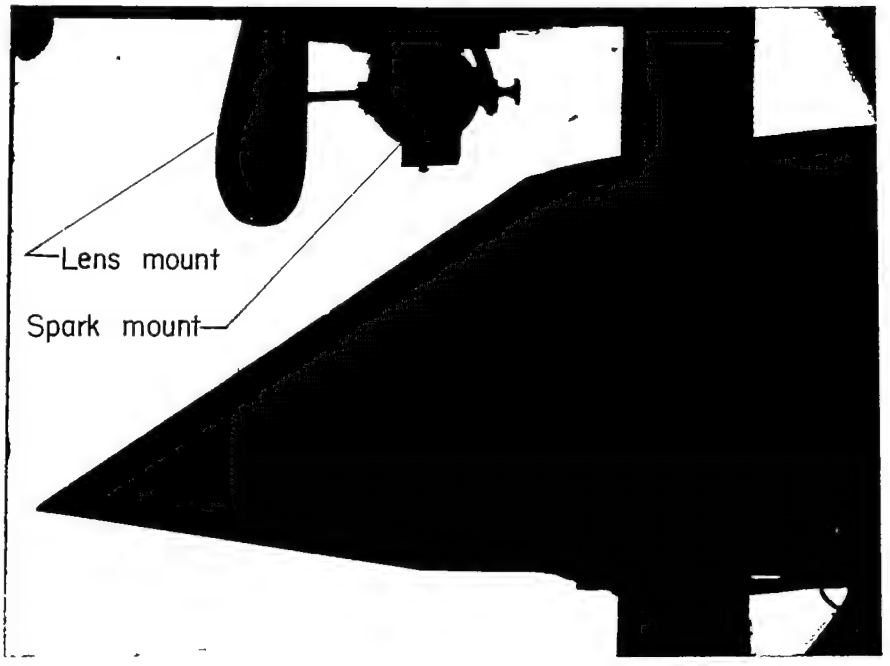

(a) No flow.

L-83676

(b) $\frac{p_b}{P_o} = 0.41$.

Figure 8.- Shadowgraphs of cascade inlet at $M_o = 3.11$.

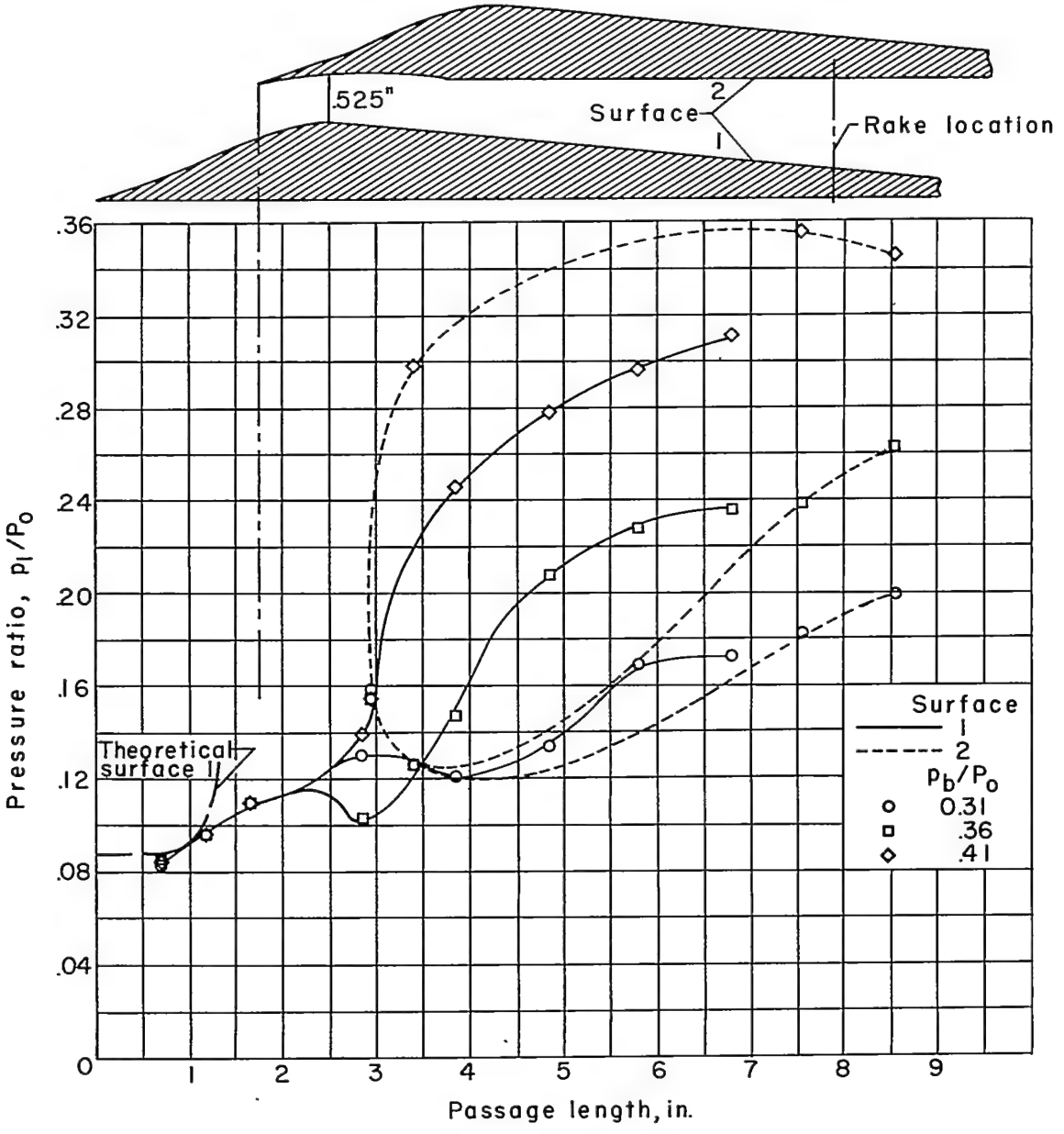

(a) Inboard passage.

Figure 9.- Cascade-inlet passage pressure distribution.

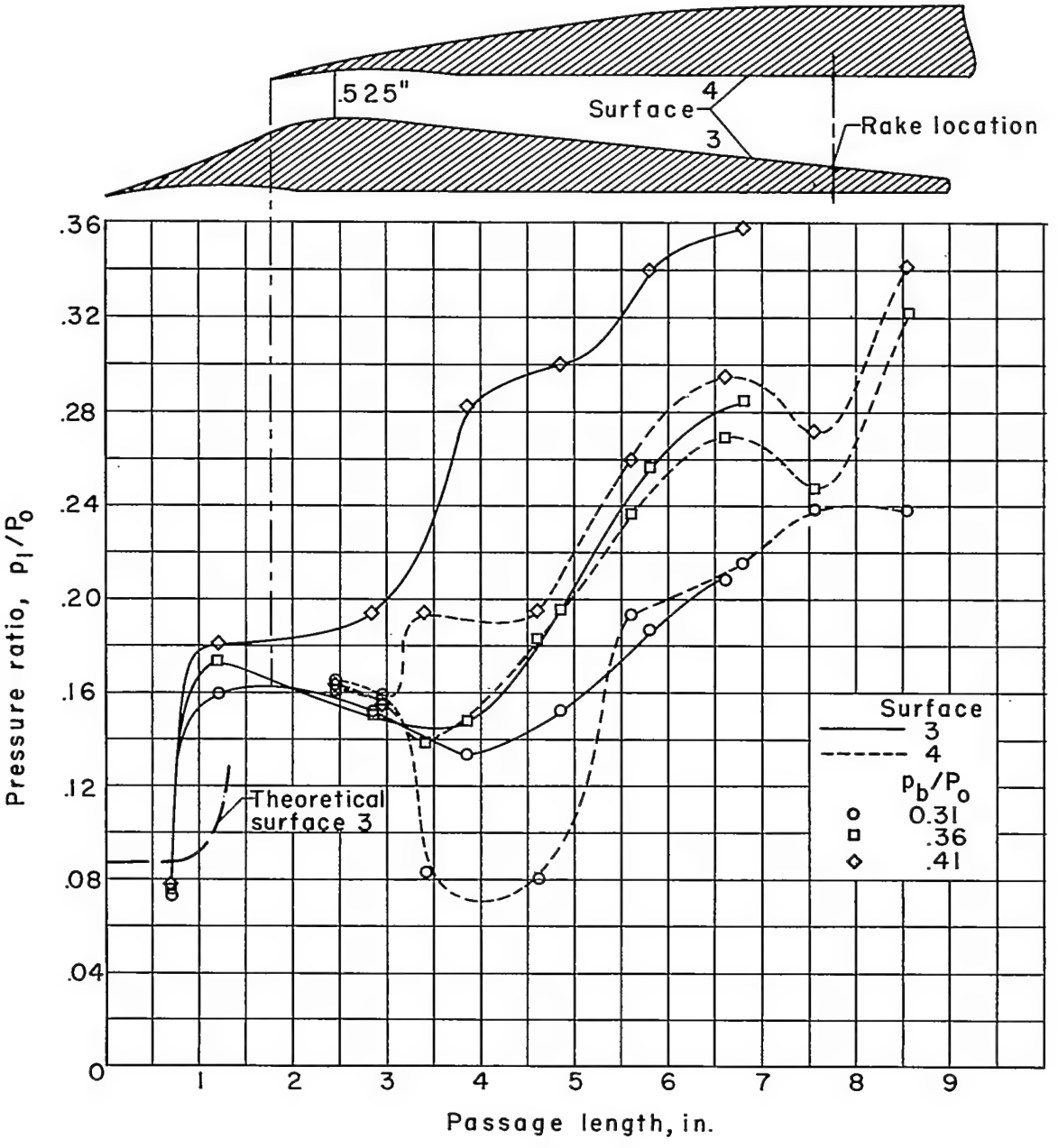

(b) Outboard passage.

Figure 9.- Concluded.

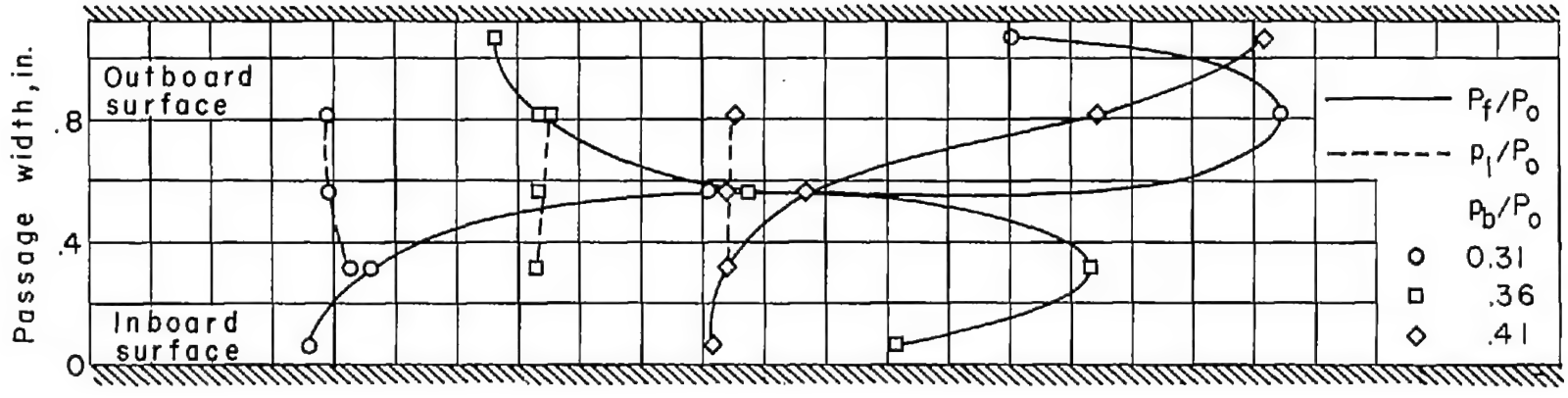

(a) Outboard passage.

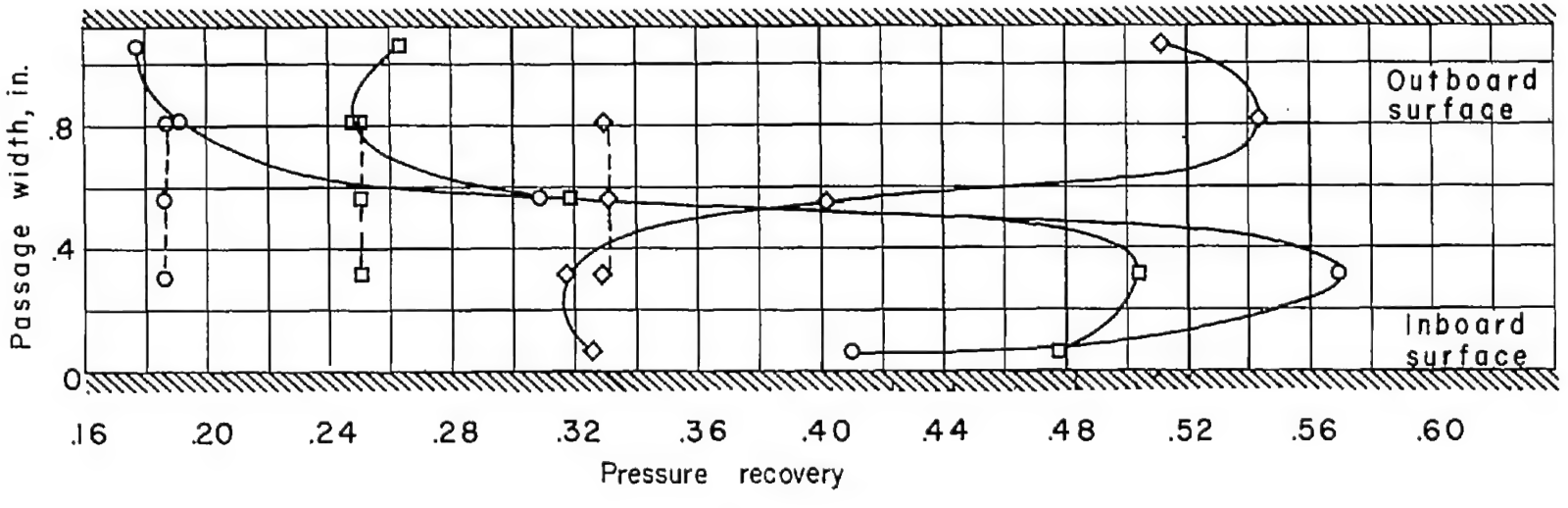

(b) Inboard passage.

Figure 10.- Cascade-inlet passage total-pressure-recovery distribution.

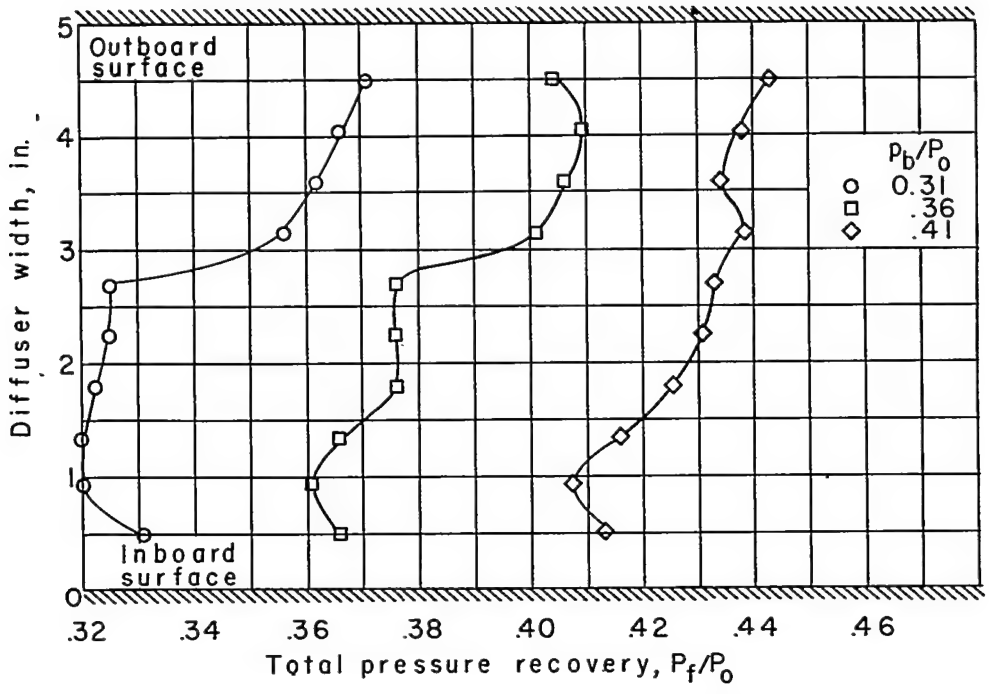

Figure 11.- Cascade-inlet total-pressure-recovery distribution in plenum chamber.

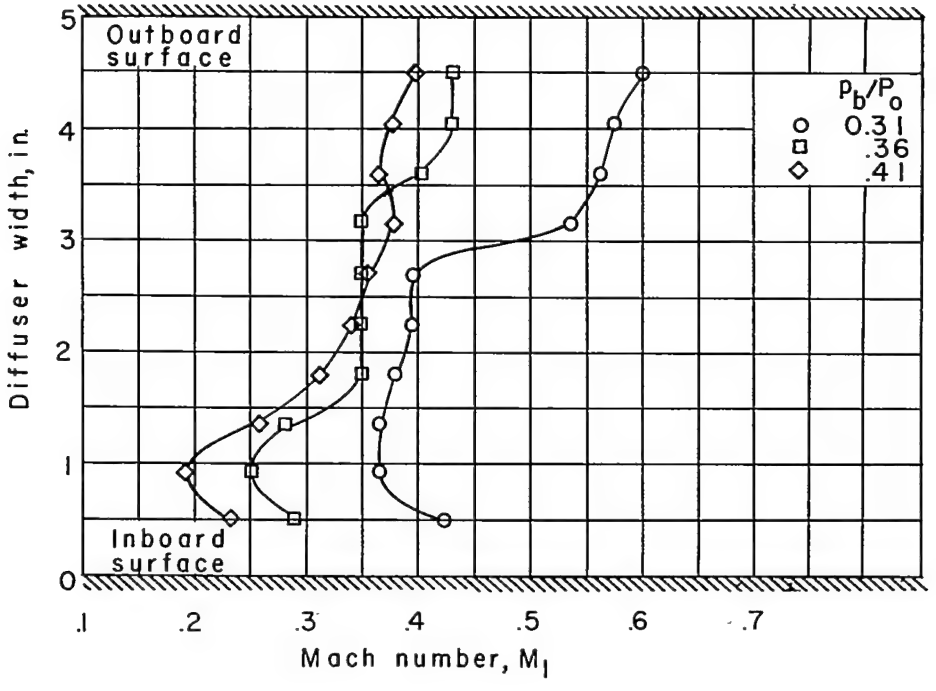

Figure 12.- Cascade-inlet Mach number distribution in plenum chamber.

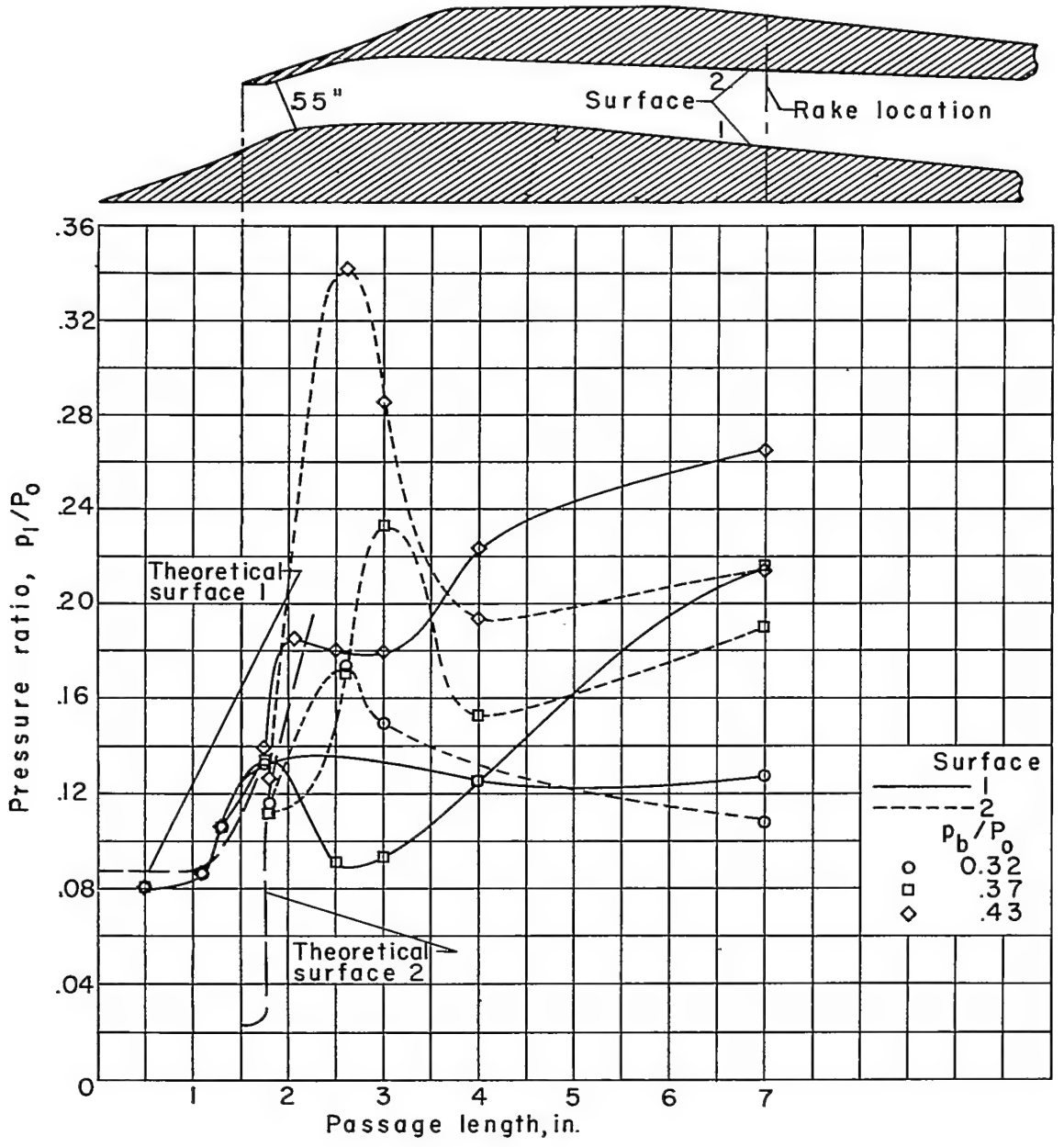

(a) Inboard passage.

Figure 13.- Stepped-cascade-inlet passage pressure distribution.

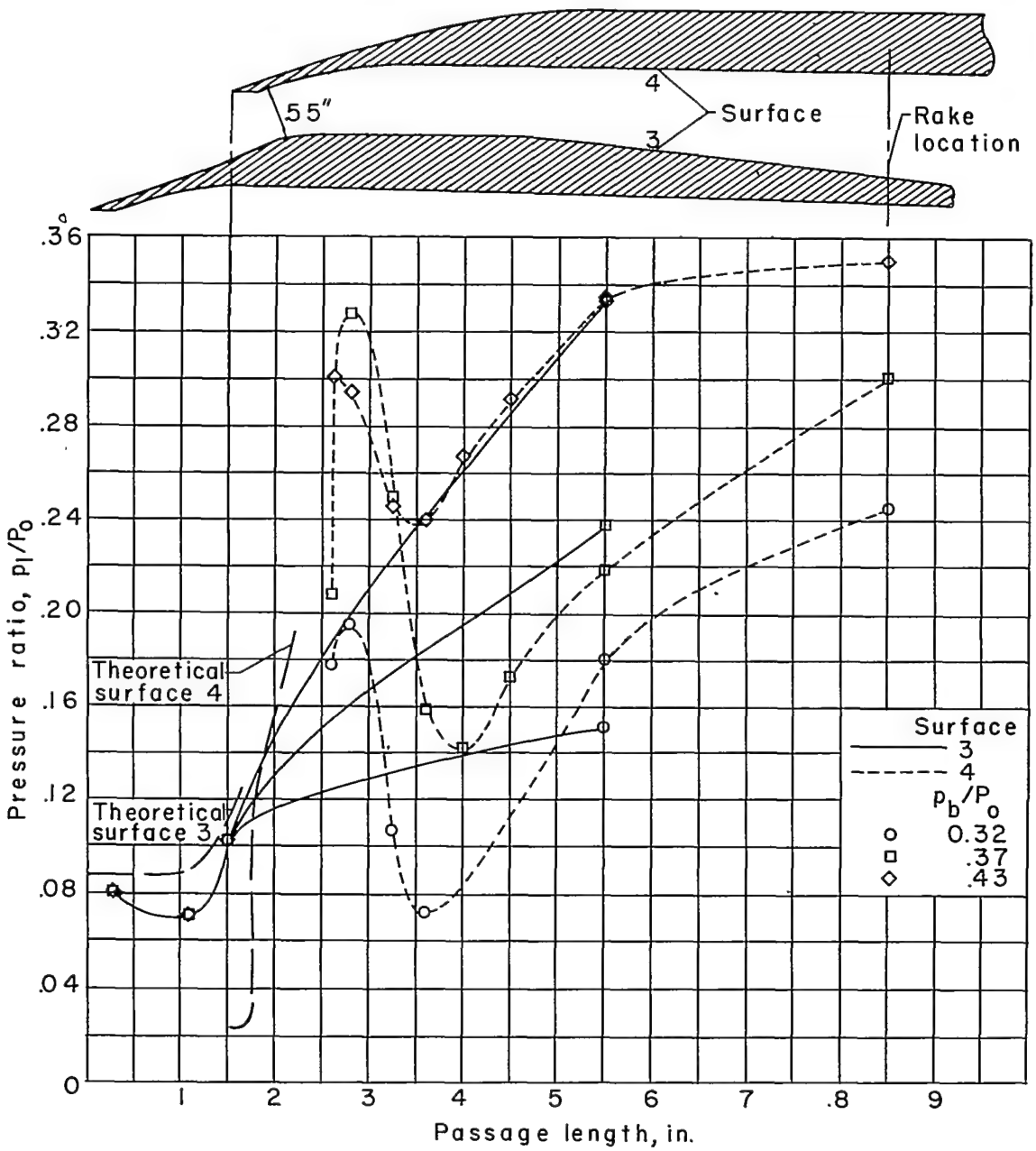

(b) Outboard passage.

Figure 13.- Concluded.

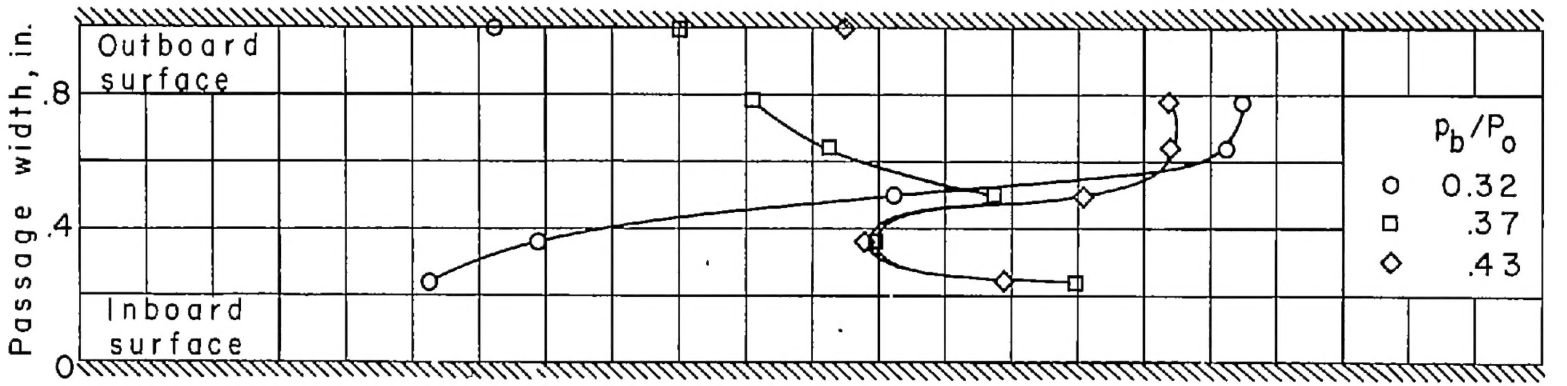

(a) Outboard passage.

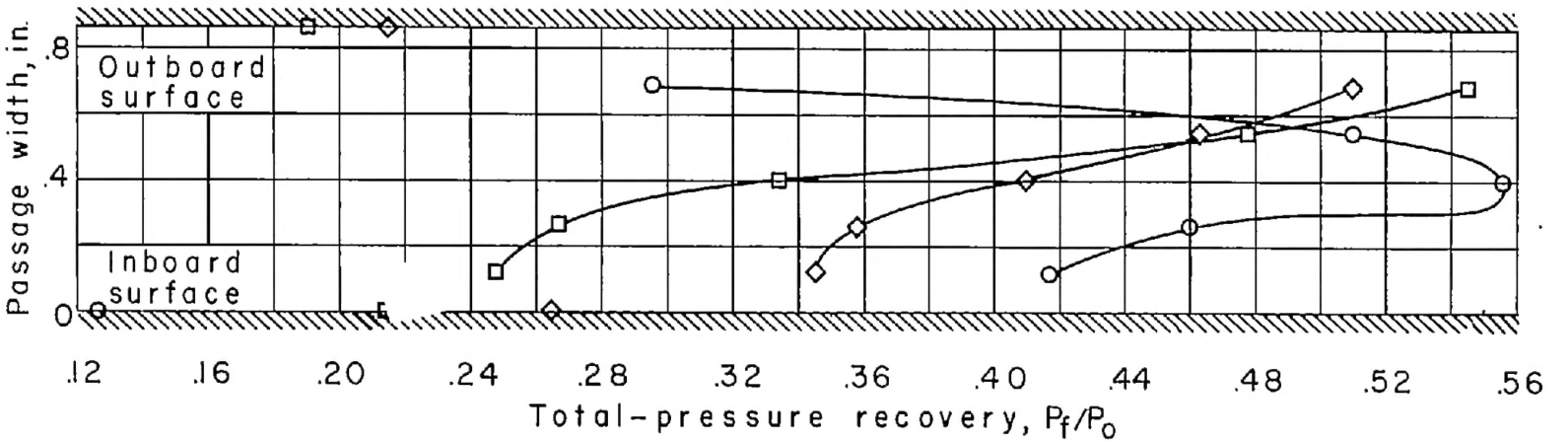

(b) Inboard passage.

Figure 14.- Stepped-cascade-inlet passage total-pressure recovery.

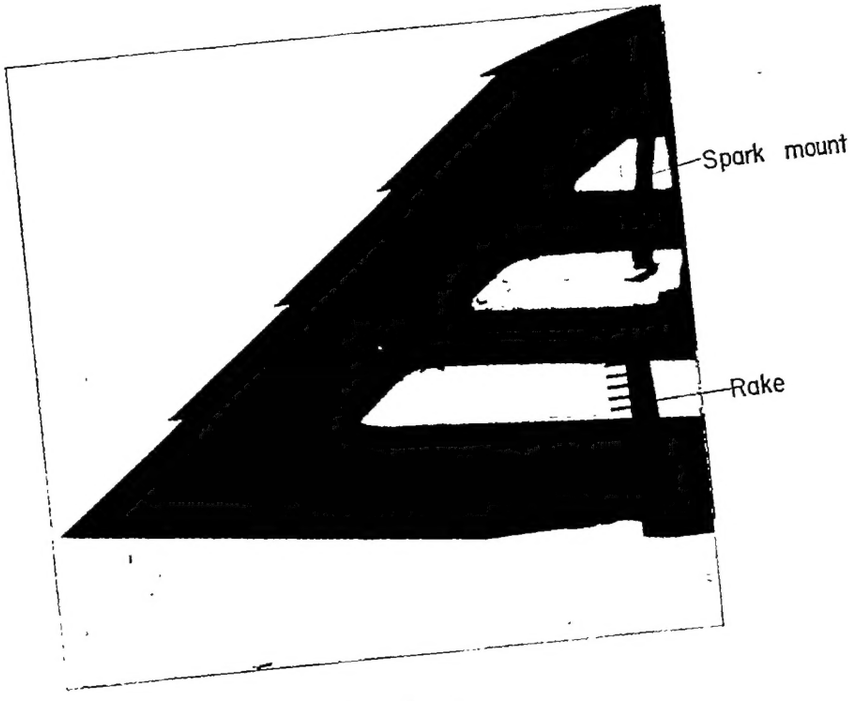

(a) No flow.

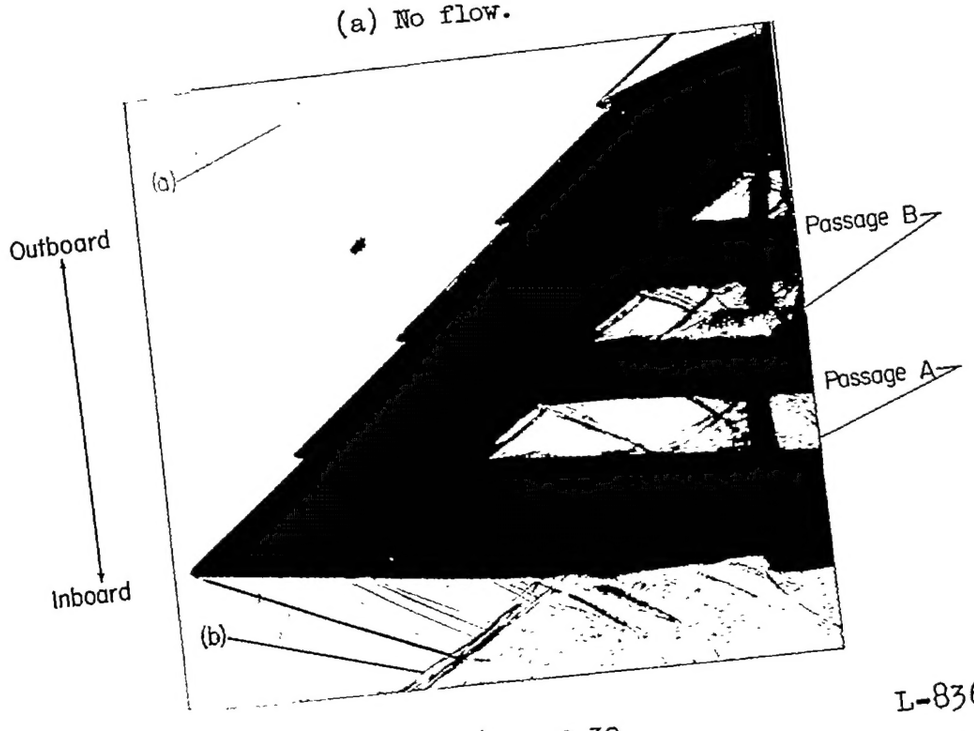

(b) $P_b/P_o = 0.32$.

Figure 15.- Shadowgraphs of stepped-cascade inlet at $M_o = 3.11$.

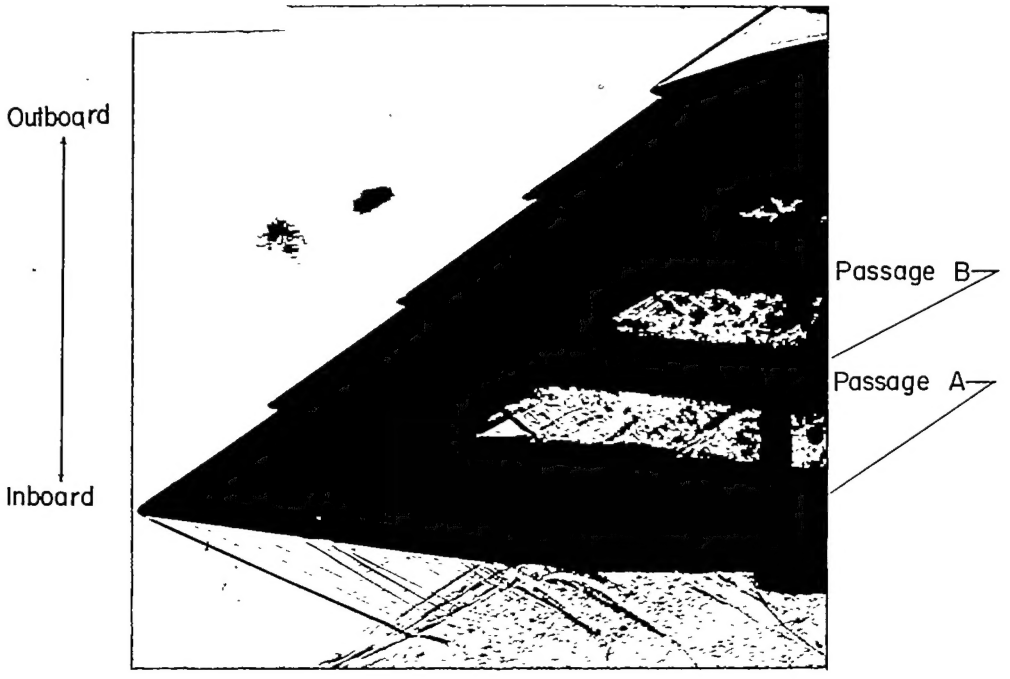

(c) $p_b/P_o = 0.37$.

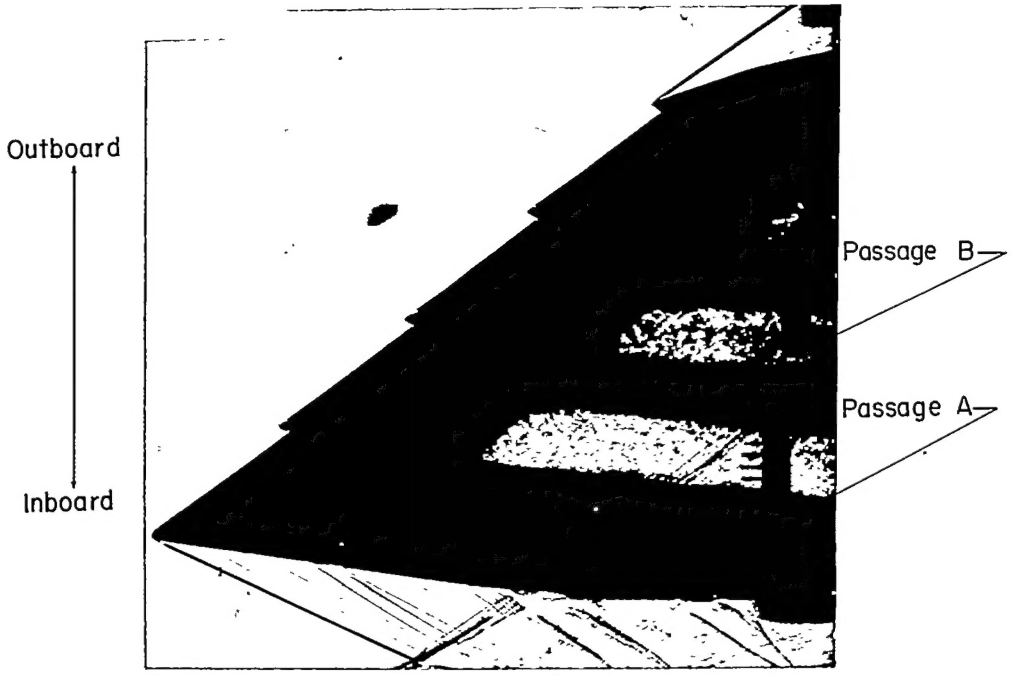

L-83678

(d) $p_b/P_o = 0.43$.

Figure 15.- Concluded.

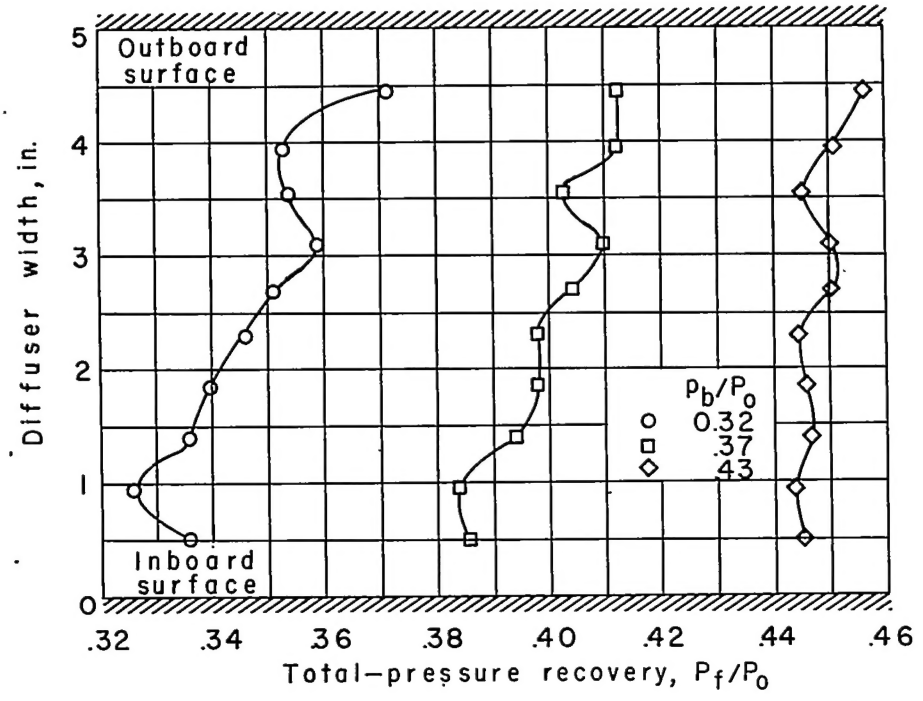

Figure 16.- Stepped-cascade-inlet total-pressure-recovery distribution in plenum chamber.

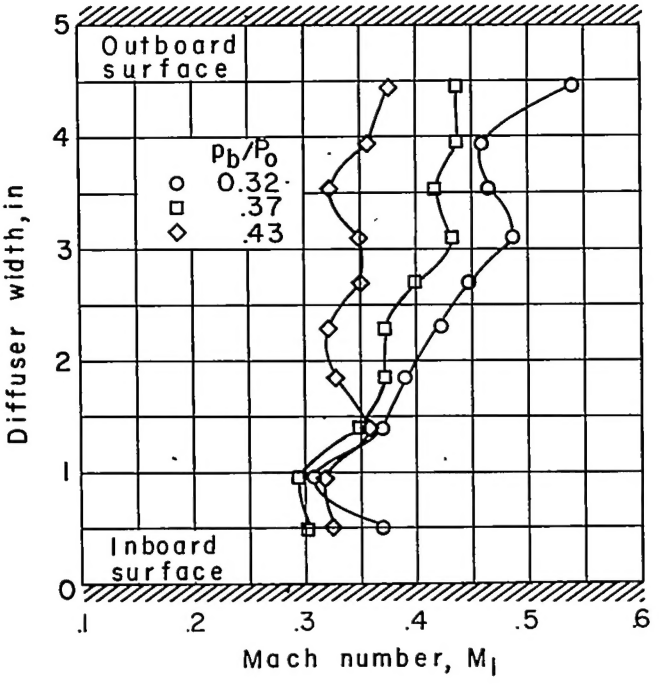

Figure 17.- Stepped-cascade-inlet Mach number distribution in plenum chamber.

NACA-Langley - 8-25-54 - 350